VEGF-A inhibits agonist-mediated Ca^{2+} responses and activation of IK_{Ca} channels in mouse resistance artery endothelial cells

Xi Ye[1], Taylor Beckett[1,2], Pooneh Bagher[1,3], Christopher J. Garland[1], Kim A. Dora[1]

Affiliations: [1]Department of Pharmacology, University of Oxford, Mansfield Road, Oxford, UK. [2]School of Biomedical Sciences, University of Queensland, Brisbane, Australia. [3]Department of Medical Physiology, Texas A&M College of Medicine, TX, USA

Joint Corresponding authors:

KA Dora, Ph.D. and CJ Garland, Ph.D.

Department of Pharmacology, University of Oxford, Mansfield Road, Oxford OX1 3QT, UK

Phone: +44 (0)1865 281114, Fax: +44(0) 1865 281114

Email: kim.dora@pharm.ox.ac.uk; christopher.garland@pharm.ox.ac.uk

Abstract word count: 174

Key points

- Prolonged exposure to VEGF-A inhibits agonist-mediated endothelial cell Ca^{2+} release and the subsequent activation of IK_{Ca} channels in mouse resistance arteries.
- Signalling via MEK downstream of VEGF-A was required to attenuate endothelial cell Ca^{2+} responses and the EDH-vasodilation mediated by IK_{Ca} activation.
- VEGF-A exposure did not modify vasodilation due to the direct activation of IK_{Ca} channels, nor the pattern of expression of IP_3 receptor 1 within endothelial cells of resistance arteries.
- These results indicate a novel role for VEGF-A in resistance arteries and suggest a new avenue for investigation into the role of VEGF-A in cardiovascular diseases.

Abbreviations

$[Ca^{2+}]_i$, intracellular calcium concentration; EC, endothelial cell; EDH, endothelium-derived hyperpolarization; ERK; extracellular-signal regulated kinase; HMVEC, human microvascular endothelial cells; HUVECs, human umbilical vein endothelial cells; IP_3, inositol trisphosphate; K_{Ca}, calcium-activated potassium channel; MAPK, mitogen-activated protein kinase; MEK, MAP/ERK kinase; NO, nitric oxide; NRP1, neuropilin-1; VEGF-A, vascular endothelial growth factor A; VEGFR, VEGF receptor; TRP, transient receptor potential; VSMC, vascular smooth muscle cell

Abstract

VEGF-A is a potent permeability and angiogenic factor that is also associated with endothelial cell (EC) activation and remodelling of the microvasculature. Elevated VEGF-A levels are linked to a significant increase in the risk of cardiovascular dysfunction, but it is unclear how VEGF-A causes these detrimental, disease related effects. Small resistance arteries are central determinants of peripheral resistance and endothelium-dependent hyperpolarization (EDH) is the predominant mechanism by which these arteries vasodilate. Using isolated, pressurized resistance arteries, we demonstrate that VEGF-A acts via VEGFR2 to inhibit both EC Ca^{2+} release and the associated EDH vasodilation mediated by IK_{Ca} channels. Importantly, VEGF-A had no direct effect against IK_{Ca} channels. Instead the inhibition was crucially reliant on the downstream activation of the MAP/ERK kinases1/2 (MEK1/2). The distribution of EC IP_3R1 was not affected by exposure to VEGF-A, and we propose an inhibition of IP_3R1 through the MEK pathway, likely ERK1/2. Inhibition of EC Ca^{2+} via VEGFR2 has profound implications for EDH-mediated dilation of resistance arteries, and could provide a mechanism whereby elevated VEGF-A contributes towards cardiovascular dysfunction.

Introduction

Vascular endothelial growth factor A (VEGF-A) is a pro-survival, angiogenic and permeability factor acting on endothelial cells (EC) (Simons, Gordon and Claesson-welsh, 2016). Although there are two receptors for VEGF-A, VEGF-A acts through VEGFR2, while VEGFR1 merely acts as a decoy receptor in ECs, at least in the context of angiogenesis (Fong *et al.*, 1995). On binding to VEGF-A, VEGFR2 dimerizes and induces the activation of a number of pathways such as MEK1/2-ERK1/2, PI3K-Akt and MKK3/4/6-p38 MAPK to initiate a range of cellular effects including DNA synthesis, proliferation and permeability (Simons, Gordon and Claesson-welsh, 2016). However, VEGFR2 dimerization appears only to explain part of the activation signal, and in some cases, amplification of the signal occurs through the recruitment and binding of VEGF-A to a co-receptor, neuropilin-1 (NRP1), enabling full activation of downstream pathways (Soker *et al.*, 1998; Kawamura *et al.*, 2008).

Although VEGF-A is thought to stimulate the generation of nitric oxide (NO) from ECs leading to arterial vasodilation (Ku *et al.*, 1993; Itoh *et al.*, 2002), the link between this signal and VEGFR is not clear. In human umbilical vein ECs (HUVECs), VEGF-A increases EC intracellular Ca^{2+} ($[Ca^{2+}]_i$) through the activation of phospholipase Cγ (PLCγ) and the subsequent production of IP_3 (Favia *et al.*, 2014). In contrast, in human microvasculature ECs (HMVECs), the increase in $[Ca^{2+}]_i$ appears not to rely on IP_3Rs, but rather Ca^{2+} influx through a receptor-operated transient receptor potential (TRP) channel (Cheng *et al.*, 2006; Hamdollah Zadeh *et al.*, 2008). An increase in EC Ca^{2+} will potentially activate NO synthase. However, to date there has been no study linking a VEGF-A evoked rise in EC Ca^{2+} and the release of NO in intact pressurized arteries.

In general, elevations in EC $[Ca^{2+}]_i$ activate at least two distinct EC-dependent vasodilator responses, one via NO release and the other due to endothelium-derived hyperpolarization (EDH) with the EDH response predominating in smaller resistance arteries (Edwards *et al.*, 1998). In the latter, an increase in EC $[Ca^{2+}]_i$ stimulates the opening of the small and intermediate conductance Ca^{2+}-activated K^+ channels (SK_{Ca}, IK_{Ca}), which are localised to the endothelium. This results in an efflux of K^+, causing hyperpolarization of the ECs. The hyperpolarizing current then spreads from the ECs to the neighbouring vascular smooth muscle cells (VSMC) via myoendothelial gap junctions, to reduce the open probability of voltage dependent Ca^{2+} channels causing vasodilation (Edwards *et al.*, 1998; Dora *et al.*, 2008). EC-dependent vasodilation helps the maintenance of blood flow and ensures sufficient oxygen and

nutrients are delivered to tissues. Reduced endothelium-dependent vasodilation occurs in a number of conditions including diabetes, cancer and peripheral arterial disease (Lim *et al.*, 2004; Stehr *et al.*, 2010; Goel and Mercurio, 2013).

In the present study, we provide evidence to suggest prolonged exposure to VEGF-A and activation of the MEK1/2 pathway lead to a reduction in EC-dependent vasodilation in mouse isolated resistance arteries, and that this reduction reflects a change in EC Ca^{2+} handling and reduced K_{Ca} opening.

Methods

Ethical approval

Ethical approval was obtained and all animal procedures were carried out in accordance with the UK Home Office Animals (Scientific Procedures) Act 1986. Experiments were carried out according to the guidelines laid down by the institution's animal welfare committee and regulations described in the *Journal of Physiology* editorial (Grundy, 2015).

Animals and tissue preparation

Wildtype male C57BL/6J mice (Charles River) between the ages of 11-16 weeks were used in this study. Animals were housed in individually ventilated cages with 12 h light/dark cycle and controlled temperature (20-22°C). Standard chow and water were available *ad libitum*. Mice were euthanized in accordance with schedule 1 of the Animals (Scientific Procedures) Act by increasing concentration of CO_2 followed by cervical dislocation as a confirmation of death. The mesentery was collected in cold MOPS buffer containing (in mM): 142.5 NaCl, 4.7 KCl, 1 $CaCl_2$, 1.17 $MgSO_4$, 3.0 MOPS, 1.2 NaH_2PO_4 (H_2O), 11.0 glucose, 2.0 pyruvate, 0.02 EDTA at pH 7.40 ± 0.02.

Artery isolation and pressure myography

Third order mesenteric resistance arteries were dissected free of adhering adipocytes and connective tissue. Arteries were cannulated onto glass micropipettes (external diameter 100-120 µm), secured with 11-0 sutures in a 2.0 mL temperature regulated chamber. Arteries were warmed to 37°C, gradually pressurized to a physiological pressure of 60 mmHg and allowed to equilibrate for 30 mins (Beleznai *et al.*, 2011). Agents were applied to the bath, except when VEGF-A was perfused into the lumen. ZM323881 or UO126 were added to the bath 20 mins

prior to perfusion of either VEGF-A and ZM323881 (VEGFR2 tyrosine kinase inhibitor) or VEGF-A and UO126 (MEK1/2 inhibitor), respectively, into the lumen of artery at 1 µL/min using a beehive syringe pump. In preliminary experiments, 250 nM carboxyfluorescein was pumped together with VEGF-A to establish the delay in delivering VEGF-A into the lumen of arteries (15 min at 1 µL/min). This time was added to the overall pumping time, meaning t=0 min was the time at which VEGF-A reached the lumen. The luminal flow was stopped immediately prior to obtaining concentration response curves.

Since the level of VEGF-A ranges from undetectable to 0.1 nM under physiological conditions (Larsson, Sköldenberg and Eericson, 2002), rising to several nanomolar in pathological situations (Baker *et al.*, 1995; Kaess *et al.*, 2016), we compared responses to 1 pM, 0.1 nM and 1 nM VEGF-A. While VEGFR2 is phosphorylated within 5 mins after VEGF-A application, activation of downstream pathways vary from 10 to 60 mins (Jang *et al.*, 2017). Therefore, arteries were perfused for 60 mins.

Diameter measurements were recorded on the stage of an inverted microscope (IX 70, Olympus, UK), attached to a confocal scanning unit (FV500, Olympus). Artery viability was assessed with contraction to 1-3 µM phenylephrine (PE) followed by endothelium-dependent vasodilation to 1-10 µM SLIGRL, a PAR2 activating peptide (McGuire *et al.*, 2002; Dora *et al.*, 2003; Beleznai *et al.*, 2011). Only arteries with dilation >90% to 3 µM SLIGRL, reflecting undamaged endothelium, were used for subsequent experiments. The outer diameter of the artery was measured using MetaMorph software (Version 7.7.4.0, Molecular Devices). % Dilation = $(D-D_{constricted})/(D_{Max}-D_{constricted})100$.

EC $[Ca^{2+}]_i$ measurement in pressurized arteries

EC Ca^{2+} investigations were conducted on third order mesenteric resistance arteries from transgenic mice on a C57Bl/6J background expressing the genetically encoded Ca^{2+} indicator, GCaMP2, under the control of a connexin40 (Cx40) promoter ($Cx40^{BAC}$-GCaMP2 Mice) (Bagher, Davis and Segal, 2011). The mesenteric artery was isolated and pressurized as described above. Ca^{2+} measurements were taken from ECs at the bottom of the pressurized artery and images were obtained using a 40x water immersion objective (40x/1.15NA objective, WD 0.25mm, Olympus; excitation 488 nm, emission >505 nm) and acquired using Olympus FluoView 1200 software (FV10-ASW) at ~3 Hz with a GaAsP detector.

Ca^{2+} data were analysed using subcellular regions of interest (ROI) as previously described (Garland *et al.*, 2017), each event categorized whilst viewing the original movie file during

manual frame-by-frame playback. If a response radiated from a single point, was synchronized, and rapidly decayed within 20 μm^2, this was termed local; Ca^{2+} waves were defined as asynchronous events that visibly propagated at least 20 µm along the length of an EC. All cells within a field of view (7-11 cells) were manually and individually analysed for Ca^{2+} event frequency. Results are presented as either frequency (events/min) or F/F_0 traces, the latter calculated by dividing the fluorescence intensity (F) by an average baseline fluorescence intensity (F_0). The number of local or propagating events were expressed as a percentage of total events.

Immunohistochemistry

Pressurized arteries were fixed with 2% paraformaldehyde for 10 mins, blocked and permeabilised with 1% BSA in PBS-Tween20 (0.1%) for 1 hour in luminal and abluminal space. Arteries were labelled with 2 µg/ml rabbit anti-IP_3R1 (PA1-901, Thermofisher Scientific) and 2 µg/ml mouse anti-ZO-1 (339-100, Thermofisher Scientific) antibodies in 1% BSA PBS-T overnight at 4°C. This was followed by 2 hours incubation with 2 µg/ml goat anti-rabbit 488 and anti-mouse 405 secondary antibodies in 1% BSA PBS-T. The nuclei and elastic lamina were labelled with 15 µM propidium iodide and 1 µM Alexa Fluor 633 hydrazide, respectively, for 20 mins. Arteries were excited at 405, 488, 546 and 633nm, the emitted fluorescence collected from cells through the bottom wall of the artery through a water immersion objective (40x) and acquired using Olympus FluoView 1000 software (FV10-ASW). Z-stacks through the wall of the artery were obtained in 0.25 µm increments and reconstructed using Imaris software (Version 5.5, Bitplane).

EC tube isolation

EC tubes were isolated as previously described (Socha *et al.*, 2011; Socha and Segal, 2013; Garland *et al.*, 2017), with modifications made to isolate from mouse mesenteric arteries. Arteries were dissected in cold dissection buffer containing (in mM): 137.0 NaCl, 5.6 KCl, 1.0 $MgCl_2$, 10.0 HEPES, 10.0 glucose, 0.01 sodium nitroprusside and 0.1% bovine serum albumin (BSA). Second and third order mesenteric arteries were dissected free of surrounding tissue. One end of the artery was cannulated onto a glass micropipette (external diameter 100-120 µm) and lumen flushed with cold dissection buffer to remove blood. Arteries were cut into 2-3 mm segments and transferred to a clear 1.5 mL microcentrifuge tube containing 1 mL cold dissection buffer. Artery segments were washed twice with enzyme free dissociation buffer

containing (in mM): 137.0 NaCl, 5.6 KCl, 1.0 $MgCl_2$, 10.0 HEPES, 10.0 glucose, 2.0 $CaCl_2$, 0.1% BSA at 37°C. Segments were then incubated in dissociation buffer supplemented with 0.62 mg/ml papain, 1.0 mg/ml dithioerythritol and 1.5 mg/ml collagenase for 20-25 mins at 37°C. Enzymatic digestion was terminated by aspiration of enzyme containing buffer and replaced with enzyme free dissociation buffer in a round culture dish for trituration. EC tubes were dissociated from surrounding vascular smooth muscle cells by gentle trituration using a glass micropipette (inner diameter 80-110 μm). A nanoliter injector (Nanoliter 2010) coupled with a Micro4 controller (World precision instruments) was mounted on an upright Olympus BX51WI microscope to allow for real-time visualization of the trituration process.

RNA extraction and RT-qPCR

Arteries and EC tubes were isolated as described above. 4 segments of second and third order artery branches from one animal were pooled for each *n*-value. Arteries were homogenised and RNA was extracted using the RNeasy plus Mini Kit (Qiagen). For EC tubes, three >1 mm long EC tubes were pooled from one animal for each *n*-value. Isolated EC tubes were transferred using a new glass micropipette into a clean round culture dish containing enzyme free dissociation buffer, and repeated three times to reduce VSMCs contamination. RNA was then extracted from EC tubes using Cells-to-CT™ 1-Step TaqMan® Kit lysis buffer (ThermoFisher Scientific) following manufacturer's instructions.

RT-qPCR were carried out using the Cells-to-CT™ 1-Step TaqMan® Kit. Pre-validated, gene specific FAM-conjugated Taqman® probes were purchased from ThermoFisher Scientific (see Table 1). Reverse transcription was performed at 50°C for 20 mins, followed by heat activation of taq polymerase at 95°C for 30 seconds. PCR was carried out by repeating 95°C for 15 s, then 60°C for 1 min for 40 cycles using the 7500 Fast Real-Time PCR system (ThermoFisher Scientific). All samples were run in duplicates along with a no template negative control for each gene. Two housekeeping genes (*Actb* and *β_2M*) were used to normalize gene expression. The relative expression was calculated using the ΔC_t method ($\Delta C_t = C_{t\,(\text{target gene})} - C_{t\,(\text{housekeeping gene})}$). Success of VSMCs removal was assessed by the expression of VSMCs marker *Acta2* (α-SMA). C_t >37 was considered not detected.

Table 1

Gene	Protein	Assay ID
Pecam-1	Platelet endothelial cell adhesion molecule-1 (PECAM-1)	Mm0124576_m1
Acta2	α–Smooth muscle actin (α–SMA)	Mm01204962_gh
β2M	β_2 microglobulin(β_2M)	Mm00437762_m1
Actb	β–actin	Mm04394036_g1
Flt1	Vascular endothelial growth factor receptor 1 (VEGFR1)	Mm00438980_m1
Flk1	Vascular endothelial growth factor receptor 2 (VEGFR2)	Mm01222435_m1
Nrp1	Neuropilin-1 (NRP-1)	Mm00435379_m1
F2rl1	Protease-activated receptor 2 (PAR2)	Mm00433160_m1
Itpr1	Inositol trisphosphate receptor 1 (IP_3R1)	Mm00439907_m1
Itpr2	Inositol trisphosphate receptor 2 (IP_3R2)	Mm00444937_m1
Itpr3	Inositol trisphosphate receptor 3 (IP_3R3)	Mm01306070_m1

Drugs

All other drugs were purchased from Sigma except mouse VEGF-A_{164} (R&D systems, #493-MV-005); Diethylamin NONOate (DEA NONOate, #82100), ZM323881 (#2475), UO126 (#1144) (Tocris); Apamin (Latoxan, #L8407), SLIGRL (Auspep). Stock solutions of ZM323881, UO126, TRAM-34 were prepared in dimethylsulfoxide (DMSO) and DEA NONOate in 10 mM NaOH. All other stock solutions were prepared in purified water.

Data analysis

All data are summarized as the mean ± SEM of *n* arteries, one per animal. The Ca^{2+} events data represent analysis of at least 7 cells per artery and values were averaged to provide one *n*-value. Only active cells were used in the calculation of frequency. Statistical comparisons were made in Prism 7 Software (GraphPad, UK) using unpaired student's t-test, one-way or two-way ANOVA with Bonferonni's post-test as appropriate. $P<0.05$ was considered significant.

Results

VEGF receptors are present in mouse resistance artery endothelial cells

RNA was extracted from either freshly isolated mesenteric arteries or from ECs alone in the form of intact EC tubes. *Pecam-1* and *Acta2* were used as EC and VSMC markers, respectively. *Pecam-1* expression was evident in both intact arteries and EC tubes, *Acta2* signal was effectively absent from EC tubes, indicating the EC samples were free from SMCs (Fig 1A). *Flt1, Flk1* and their co-receptor *Nrp1* were each expressed in the EC tubes (Fig 1B). Despite the presence of VEGF receptors and functional endothelium, luminal perfusion of 0.1 nM or 1 nM VEGF-A did not result in vasodilation of arteries constricted with the α_1-adrenoceptor agonist phenylephrine (PE) (Fig 1C).

VEGF-A inhibits EDH-mediated vasodilation to SLIGRL

We investigated whether prolonged luminal exposure to 1 nM VEGF-A, a concentration known to effectively to activate VEGFR2 in rat arteries (Itoh *et al.*, 2002; Egholm *et al.*, 2016), can alter endothelium-dependent vasodilation to other agonists in small resistance arteries. SLIGRL readily dilates mouse resistance arteries via the EDH-pathway, and to a lesser extent, NO (McGuire *et al.*, 2002; Beleznai *et al.*, 2011). Perfusion of 1 nM VEGF-A for 60 mins right-shifted the concentration response curve to SLIGRL by >2.5-fold (log EC_{50} -5.37 ± 0.02, n = 12) compared to vehicle (log EC_{50} -5.79 ± 0.01, n = 8), an effect that was not evident when arteries were perfused with 1 pM or 0.1 nM VEGF-A (Fig 2A). The maximum dilation to SLIGRL was not affected by 1 nM VEGF-A (E_{Max} 99.9 ± 0.1%, n = 12; vehicle: 99.6 ± 0.4%, n = 8).

To establish whether VEGF-A was affecting the NO and/or EDH pathway, the NO synthase inhibitor L-NAME was used. L-NAME had no effect on SLIGRL-mediated dilation either when added alone or in the additional presence of VEGF-A (Fig 2B), showing that inhibition of the NO pathway cannot account for the inhibition of SLIGRL-mediated vasodilation by 1 nM VEGF-A. Direct relaxation of VSMCs using the NO donor, DEA NONOate was also unaltered by VEGF-A (Fig 2C).

Since EC IK_{Ca} and SK_{Ca} channel activation underlies EDH-evoked vasodilation, their role was explored using NS309, a positive modulator of both channels. We tested the selectivity of NS309 to mediate vasodilation via IK_{Ca} and SK_{Ca} channels using TRAM-34 and Apamin (Fig

2D) and found that at 1 µM, NS309-mediated vasodilation is solely dependent on IK_{Ca} and SK_{Ca} opening. About 70% of the vasodilation to NS309 was inhibited by IK_{Ca} and SK_{Ca} blockade at 3 µM, and a significant level of vasodilation was independent of the K_{Ca} channels at 10 µM (Fig 2D). Vasodilation to NS309 was not altered by VEGF-A at 1 and 3 µM NS309 (Fig 2D), suggesting the target may be upstream of EC K_{Ca} channels.

The effect of inhibition of IK_{Ca} and/or SK_{Ca} channels was then assessed with 1 µM TRAM-34 and 100 nM apamin, respectively. Blocking IK_{Ca} with 1 µM TRAM-34 reduced the EDH component of SLIGRL-mediated vasodilation to a level similar to VEGF-A perfusion alone (Fig 3A). TRAM-34 also attenuated SLIGRL-mediated vasodilation following VEGF-A perfusion, but the effect was noticeably smaller compared to the vehicle perfused artery. The inhibitory effect against SLIGRL-mediated vasodilation was greater with the combined treatment of VEGF-A perfusion and TRAM-34 than with VEGF-A alone. In contrast, SK_{Ca} inhibition with apamin did not affect SLIGRL-mediated dilation in the vehicle control group, but markedly inhibited vasodilation in VEGF-A treated arteries, more effectively than with VEGF-A and TRAM-34 (Fig 3B). Thus, when SK_{Ca} channels are blocked and EDH-vasodilation to SLIGRL relies only on IK_{Ca} activation, VEGF-A had a pronounced inhibitory effect. When both IK_{Ca} and SK_{Ca} were inhibited, vasodilation to SLIGRL was significantly reduced compared with inhibition of either IK_{Ca} or SK_{Ca} channels alone, consistent with vasodilation occurring via EDH. Under these conditions, the ability of VEGF-A to inhibit SLIGRL-mediated vasodilation was lost (Fig 3C, 3D).

EC Ca^{2+} signalling was inhibited by VEGF-A exposure

Consistent with our previous studies, SLIGRL increased whole cell EC Ca^{2+} in pressurized murine mesenteric arteries associated with propagating waves (Fig 4A). In vehicle-perfused control arteries, EC Ca^{2+} events developed locally then propagated along the cell (Ca^{2+} waves) (Fig 4A). In contrast, luminal perfusion with 1 nM VEGF-A prevented local Ca^{2+} from evolving into more propagating events (Fig 4, 5A, D). By examining each Ca^{2+} event separately, we observed the wave events propagating at least 20 µm from where the Ca^{2+} originated in the vehicle perfused arteries, but such propagation was absent in the VEGF-A treated arteries in response to 3 µM SLIGRL (Fig 5A).

Overall, VEGF-A had a marked effect on the profile of Ca^{2+} events evoked by SLIGRL, reducing the number of active cells, the frequency of Ca^{2+} events and Ca^{2+} waves (Fig 5).

VEGFR2-MEK1/2 signalling is necessary for inhibition of both SLIGRL-mediated vasodilation and EC Ca^{2+}activity

To identify the mechanism responsible for attenuating EDH-mediated vasodilation, either 10 nM ZM323881, a selective VEGFR2 tyrosine kinase inhibitor (Whittles *et al.*, 2002), or 10 µM UO126 (Boscolo, Mulliken and Bischoff, 2011), a selective blocker of MEK1/2 were used. The concentration of ZM323881 and UO126 used have been demonstrated to selectively inhibit VEGFR2 and MEK1/2, respectively (Whittles *et al.*, 2002; Tran and Neary, 2006; Boscolo, Mulliken and Bischoff, 2011). In each case the inhibitory effects of VEGF-A on EC Ca^{2+} handling and vasodilation were prevented (Fig 6A-D), consistent with a central role for ERK1/2 downstream of VEGFR2 in the regulation of EC Ca^{2+} and the subsequent vasodilation in response to SLIGRL.

IP_3R1 distribution in ECs

The expression of *Itpr1-3* were found in freshly isolated intact arteries and EC tubes (Fig 7A). IP_3R1 within ECs appeared as punctate strings forming a net-like arrangement across the cells and along the cell borders. Clusters of IP_3R1 were sometimes observed. There was no obvious change in IP_3R1 distribution following 60 min perfusion with vehicle or 1 nM VEGF-A (Fig 7B). ZO-1 was used to distinguish the EC cell border and junctional integrity, and there was no change in ZO-1 distribution following VEGF-A perfusion.

Discussion

This study provides evidence that prolonged stimulation with VEGF-A, through the activation of VEGFR2 and the MEK1/2 pathway, inhibits EC Ca^{2+} mobilisation and agonist evoked vasodilation in mouse mesenteric resistance arteries. The altered Ca^{2+} handling prevented the effective activation of EC K_{Ca} channels, in particular IK_{Ca}, reducing the subsequent EDH-mediated vasodilation.

The majority of studies on the arterial action of VEGF-A have focussed primarily on its acute role as a vasodilator. Longer term effects of VEGF-A have not been reported, despite the fact that VEGF-A is elevated chronically in numerous pathological conditions, including peripheral artery disease, diabetes associated complications and pre-eclampsia (Baker *et al.*, 1995; Stehr *et al.*, 2010). Furthermore, high serum VEGF-A has been linked to an increased likelihood of detrimental cardiovascular events (Kaess *et al.*, 2016). Most studies rely on an antibody based

enzyme linked immunosorbent assay (ELISA) to detect VEGF-A in the blood. However, both the type of sample (serum/plasma) and the circulating levels of soluble VEGFR1 and VEGFR2 affect VEGF-A binding to antibodies and as such reduce our ability to accurately determine the concentration of circulating VEGF-A. Thus, the reported normal level for VEGF-A in the blood ranges from undetectable to about 100 picomolar, values that can increase into the nanomolar range in cancer and pre-eclampsia patients (Baker *et al.*, 1995; Takahashi *et al.*, 1995; Larsson, Sköldenberg and Eericson, 2002). In the present study, we used 1 nM VEGF-A, which is known to effectively activate VEGFR2 and mediate vasodilation in a number of different vascular beds (Itoh *et al.*, 2002; Egholm *et al.*, 2016).

Using a previously established method to isolate fresh ECs rapidly from mesenteric arteries (Socha *et al.*, 2011), we detected both VEGFRs and NRP-1 expression, confirming the presence of VEGF receptors in the ECs of resistance arteries. However, despite the presence of a functional endothelium and VEGFRs, we were unable to evoke vasodilation with VEGF-A in mouse mesenteric arteries. VEGF-A level rises gradually with perfusion, with the concentration peaking about 5 minutes following the start of VEGF-A arrival in the lumen. Vasodilation was not observed at any point, suggesting neither the low or high concentration of VEGF-A led to vasodilation of mouse mesenteric arteries. In other vascular beds, VEGF-A evoked vasodialtion is slow, often requiring 10-15 mins before vasodilation is observed, and appears to be NO-dependent. As we found that exogenous NO only evoked moderate vasodilation of mouse mesenteric arteries, the lack of vasodilation to VEGF-A may simply reflect a lack of responsivness in this artery.. Although it has been reported that when NOS is inhibited, VEGF-A can instead cause vasoconstriction (Egholm *et al.*, 2016), we did not observe this phenomenon.

In spite of a low arterial sensitivity to NO, SLIGRL evoked pronounced EC-dependent vasodilation via EDH (McGuire *et al.*, 2002). This vasodilation was inhibited following 60 mins exposure to VEGF-A, showing the growth factor can negatively and significantly attenuate EDH-vasodilation. The inhibitory action of VEGF-A did not increase further during repeated dose response curves approximately an hour later in the presence of L-NAME. This ability of VEGF-A to reduce vasodilation does not appear to be restricted to SLIGRL, others have observed reduced vasodilation to bradykinin using human dermal resistance arteries (Svedas *et al.*, 2003). Supporting an inhibitory action against vasodilation as a general

mechanism, high dose VEGF-A infusion causes a sustained increase in systemic vascular resistance (Yang *et al.*, 1998).

SLIGRL-evoked vasodilation in mesenteric arteries from wildtype mice relies on EDH, which is mediated by K^+ efflux through EC IK_{Ca} and SK_{Ca} channels (Dora *et al.*, 2003; Beleznai *et al.*, 2011). However, VEGF-A did not alter vasodilation to the K_{Ca} channel opener NS309, a positive modulator of the channels that mimics EDH-vasodilation. As NS309 activates both SK_{Ca} and IK_{Ca} channels, this raised the possibility VEGF-A modifies the input of only one type of channel. EC SK_{Ca} inhibition with apamin had a profound effect on SLIGRL-mediated vasodilation, but only following exposure to VEGF-A, suggesting the growth factor targets IK_{Ca}, to explain the attenuation in vasodilation. Interestingly, TRAM-34 right-shifted the SLIGRL (control) vasodilation curve, indicating a predominant role for these channels for EDH-vasodilation, and contrasting with the absence of a similar shift when SK_{Ca} channels were blocked with apamin. Following VEGF-A perfusion, there remained a small EDH component sensitive to TRAM-34 inhibition. Suggesting VEGF-A did not completely abolish IK_{Ca} response. EDH-vasodilation was abolished by combined block of IK_{Ca} and SK_{Ca}, and not surprisingly there was no inhibitory effect with VEGF-A, highlighting EDH as the target for VEGF-A mediated attenuation.

Boeldt *et al* had previously reported VEGF-A can affect connexion 43 (Boeldt *et al.*, 2017), which can inhibit the propagation of EDH to mediate vasodilation. However, The fact that NS309-mediated vasodilation was not modified at all by VEGF-A suggests current propagation and the EC K_{Ca} channels may not be the primary target for VEGF-A attenuation. This raised the possibility that the inhibitory target was downstream of PAR2 receptor activation but upstream of K_{Ca} channels. SLIGRL acts through PAR2 to induce Ca^{2+} release via IP_3Rs, with these Ca^{2+} events evolving into propagating waves spreading across the ECs. However, following exposure to VEGF-A, the number of cells responding to SLIGRL was reduced and the underlying Ca^{2+} events became localised to smaller more restricted sites. The restriction of Ca^{2+} release after exposure to VEGF-A translated to a reduced global increase of Ca^{2+}, which would be predicted to compromise the effective opening of EC K_{Ca} channels and thus reduce EDH-vasodilation. Although it is likely that both IK_{Ca} and the SK_{Ca} channels are affected by the reduction in Ca^{2+} release, the reduction appeared particularly pronounced with IK_{Ca} input to EDH, because once SK_{Ca} channels were inhibited by apamin the ability of SLIGRL to fully dilate arteries was dramatically reduced by VEGF-A. The greater impact of IK_{Ca} block is most

likely due to the fact these channels are localised in the fine myoendothelial projections, where ECs make contact with the VSMCs, whereas the SK_{Ca} channels are more uniformly distributed across the membrane (Dora *et al.*, 2008). Others have reported that in HUVECs, 250 pM VEGF-A reduced the ATP-mediated increase in frequency of Ca^{2+} bursts and $[Ca^{2+}]_i$ (Boeldt *et al.*, 2017). Therefore, it appears the effects of VEGF-A are not limited to PAR2-receptor mediated responses.

MEK1/2 signalling (and subsequent activation of ERK1/2) is a major signalling pathway downstream of VEGFR2 activation and it appears to be essential for VEGF-A to exert an inhibitory effect on EC Ca^{2+} release. This suggests ERK1/2, a serine/threonine kinase, may have a direct role in the regulation of EC Ca^{2+}. Other studies suggest that ERK phosphorylates S^{436} of IP_3R1, to reduce Ca^{2+} release and the frequency of Ca^{2+}oscillations (Bai et al., 2006). This ERK1/2 phosphorylation site is absent in both IP_3R2 and 3 (Bai *et al.*, 2006; Yang *et al.*, 2006), which supports the possibility that SLIGRL-mediated Ca^{2+} release and propagation is largely dependent on IP_3R1 in our study. When we examined the localisation and distribution of IP_3R1, we did not observe any obvious changes, so it is unlikely that alterated Ca^{2+} signalling was caused by a redistribution of IP_3R1. However, once appropriate phospho-specific antibodies to IP_3R1 become available for immunolabelling, it will be interesting to establish if the IP_3R1 is phosphorylated during exposure to VEGF-A in pressurized artery ECs, and on which residues.

Our understanding of VEGF-A signalling in the resistance vasculature is far from complete. The majority of data available have focussed on capillaries and the ability of VEGF-A to evoke arterial vasodilation. Due to its angiogenic and pro-survival properties in ECs, VEGF-A has been trialled for therapeutic re-vascularisation. Although early studies suggest VEGF-A improves myocardial outcome in patients, the benefits of this approach were far less clear in later, more stringent trials (Losordo *et al.*, 2002; Stewart *et al.*, 2009). While others have suggested VEGF-A may reduce NO release evoked by other EC-dependent vasodilators in vitro (Boeldt *et al.*, 2017), our study provides the first functional evidence to suggest that long term exposure to VEGF-A prevents effective vasodilation and that it does this by disrupting EDH-vasodilation. As such, VEGF-A has the potential to increase peripheral resistance and compromise tissue blood flow, which may counteract any potential benefit of therapeutic angiogenesis.

Author contribution

X.Y. conceived and designed the work and drafted the manuscript. X.Y and T.B acquired, analysed and interpreted the data. P.B., C.J.G. and K.A.D. helped design and interpret experiments and edited the manuscript. All authors approved the final version of the manuscript.

Funding

This work was supported by the British Heart Foundation (PG/14/58/30998; FS/13/16/30199) and the Oxford BHF Centre of Research Excellence (RE/13/1/30181). K.A.D. is a BHF-funded Senior Basic Science Research Fellow.

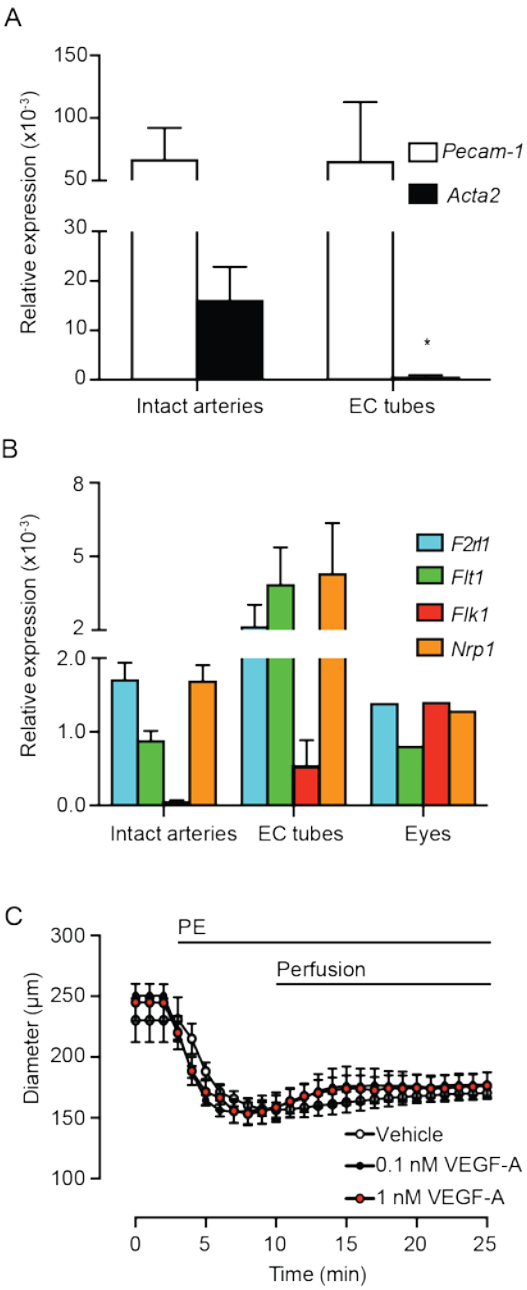

Fig 1. VEGF-A receptor expression in mouse mesenteric resistance arteries. *A.* Pecam-1 and Acta2 expression in intact arteries and isolated EC tubes. *B.* Flt1, Flk1 and Nrp1 expression (n = 4 animals). Eyes from a asingle aimal were used as a positive control for the VEGF-A receptors. *C.* Arteries were pre-constricted with PE. When pumped into the lumen of arteries, neither vehicle nor VEGF-A dilated the artery within 15 min (n = 3-4). *P<0.05 compared with intact arteries.

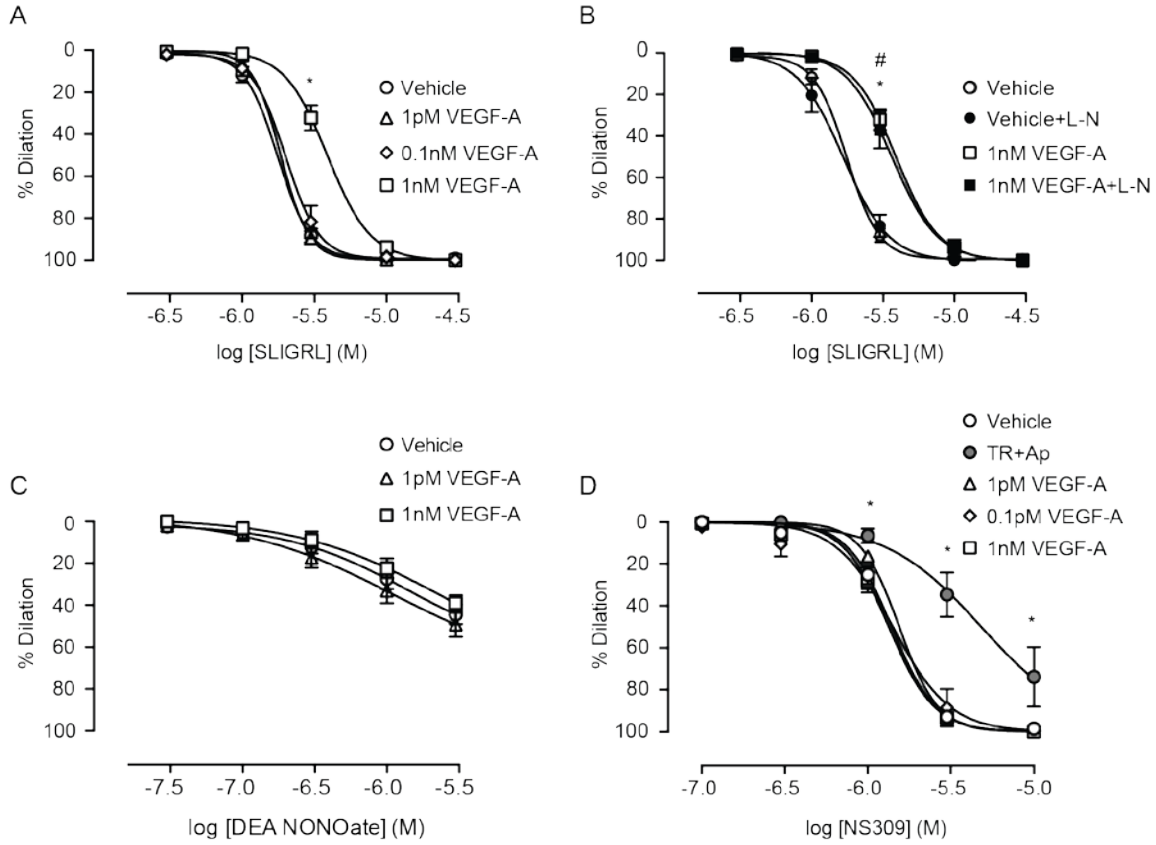

Fig 2. VEGF-A inhibits EDH-mediated vasodilation evoked by SLIGRL. Arteries were perfused with either vehicle or VEGF-A for 60 min. *A.* Vasodilation to SLIGRL (*n* =7-8). *B.* Vasodilation to SLIGRL in the presence of L-NAME (L-N, *n* = 5-8). *C.* Vasodilation to DEA NONOate (*n* = 7-9). *D.* Vasodilation to NS309 (*n* = 3-12). **P*<0.05 compared with vehicle. #*P*<0.05 compared with vehicle+L-N.

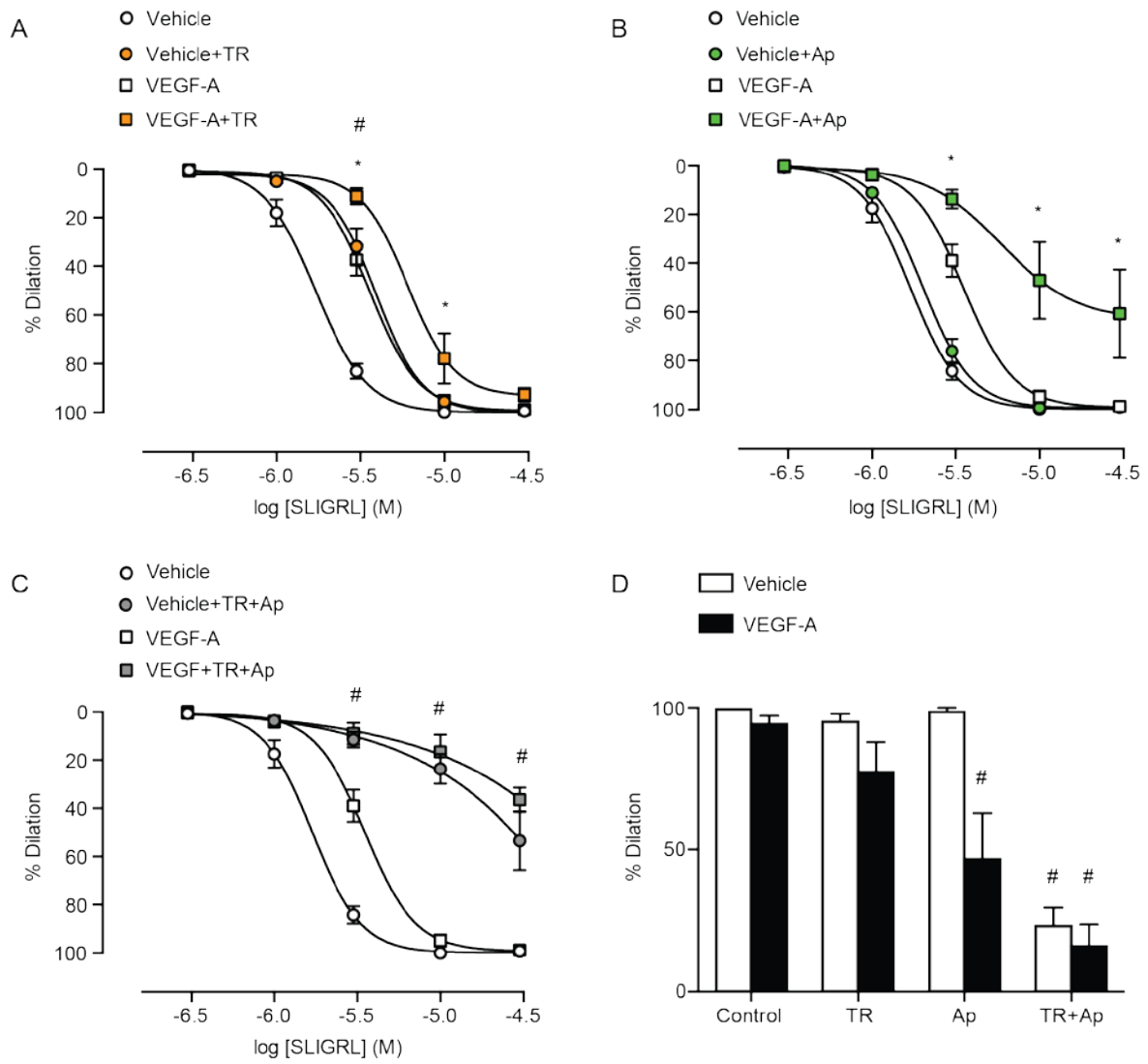

Fig 3. VEGF-A inhibits IKCa and SKCa dependent EDH vasodilation. Arteries were perfused with either vehicle or 1 nM VEGF-Afor 60 min. All experiments were performed in the presence of L-NAME. Vehicle and VEGF-A are from Fig 2. *A.* Vasodilation to SLIGRL with the addition of TRAM-34 (*n* = 5-13). *B.* Vasodilation with the addition of apamin (*n* = 3-13). *C.* SLIGRL-mediated vasodilation in the presence of TRAM-34 and apamin (*n* = 3-13). *D.* Vasodilation ot 10 µM SLIGRL in the presence of IK_{Ca} and SK_{Ca} inhibitors. **P*<0.05 compared with VEGF-A, #*P*<0.05 compared with vehicle+TR.

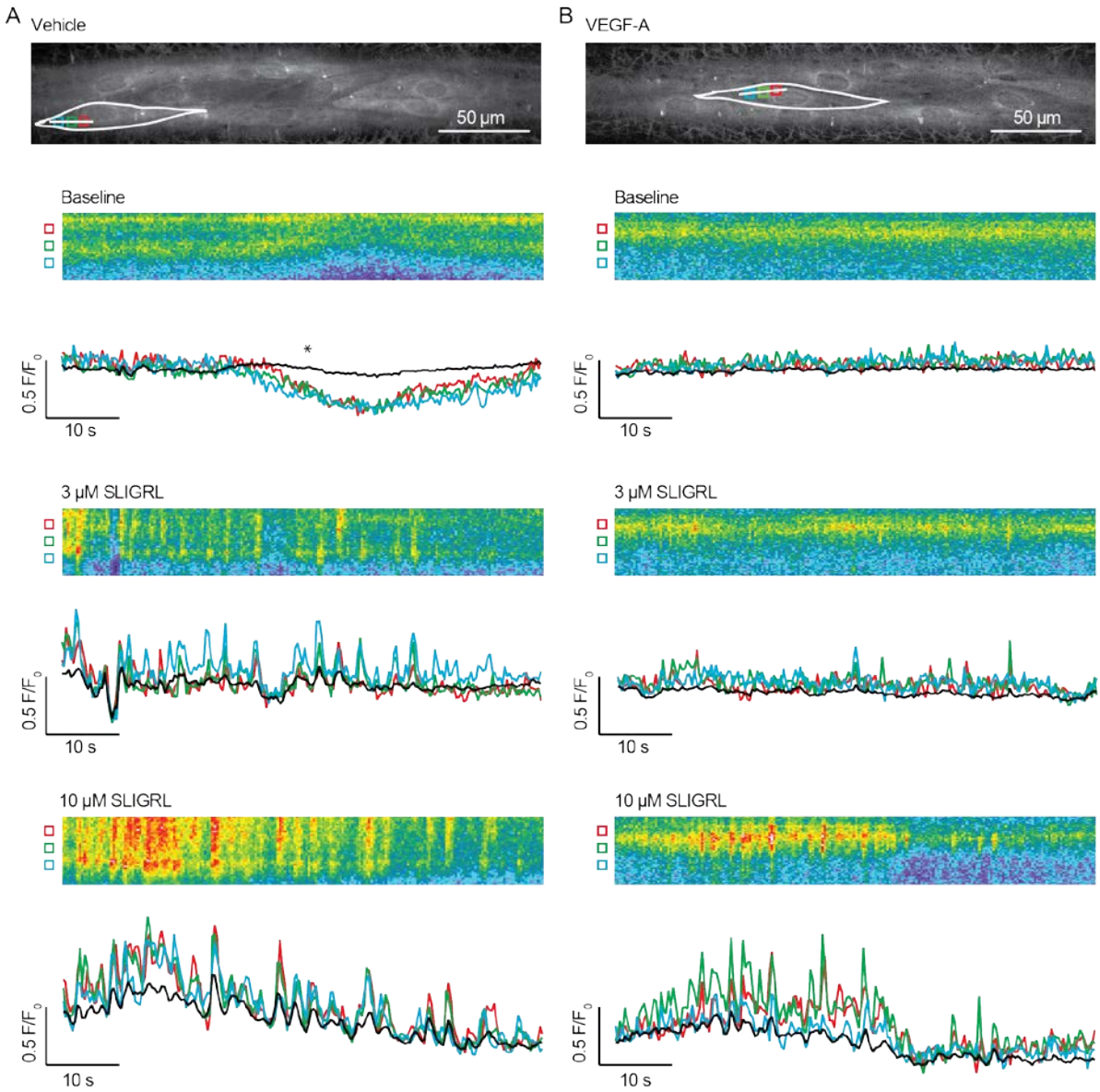

Fig 4. VEGF-A pre-exposure inhibits propagation of EC Ca^{2+}. Pressurized arteries were luminally perfused with vehicle or 1 nM VEGF-A for 60 min. Baseline Ca^{2+} was recorded for 1 min, SLIGRL was then added and remained in the bath for the duration of the recording. *A.* Following perfusion of vehicle, 3 µM and 10 µM SLIGRL stimulated a clear increase in Ca^{2+} waves along the length of the cell. *B.* Following perfusion of VEGF-A, 3 µM SLIGRL stimulated less frequent, localized Ca^{2+} events, where as 10 µM SLIGRL increased Ca^{2+} event frequency, and Ca^{2+} waves propagated along the cell. Data displayed as line-scans (corresponding to white lines in A and B) with fluorescent traces referring to subcellular regions of interest (coloured boxes in A and B). Black trace refers to whole-cell recording. *Dip in intensity due to movement artefact. Representative of 5-6 independent experiments.

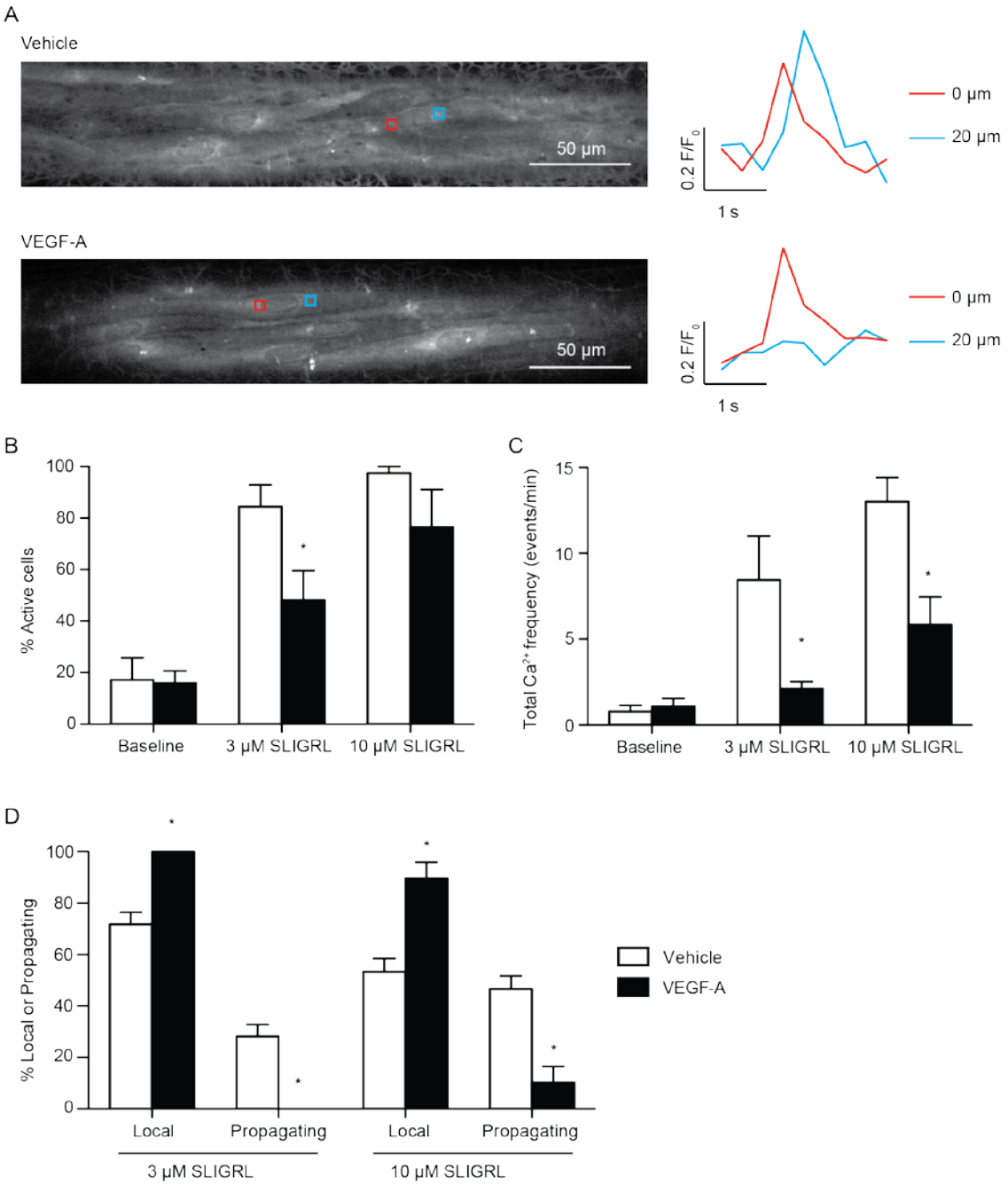

Fig 5. VEGF-A inhibits SLIGRL-mediated Ca^{2+} events and wave propagation. *A.* Arteries were stimulated with 3 µM SLIGRL. Regions of interests were positioned 20 µm apart in active ECs. (*Upper*) vehicle perfused; (*Lower*) 1 nM VEGF-A perfused. Representative of 5-6 independent experiments. Summary of Ca^{2+} events. Following luminal perfusion with 1 nM VEGF-A for 60 min, fewer ECs respond to 3 µM SLIGRL (*B*) and of the active cells, there were fewer Ca^{2+} events (*C*). *D.* VEGF-A treated arteries produced fewer propagating Ca2+ events compared with the vehicle treated arteries. n = 5-6; **P*<0.05 compared with vehicle.

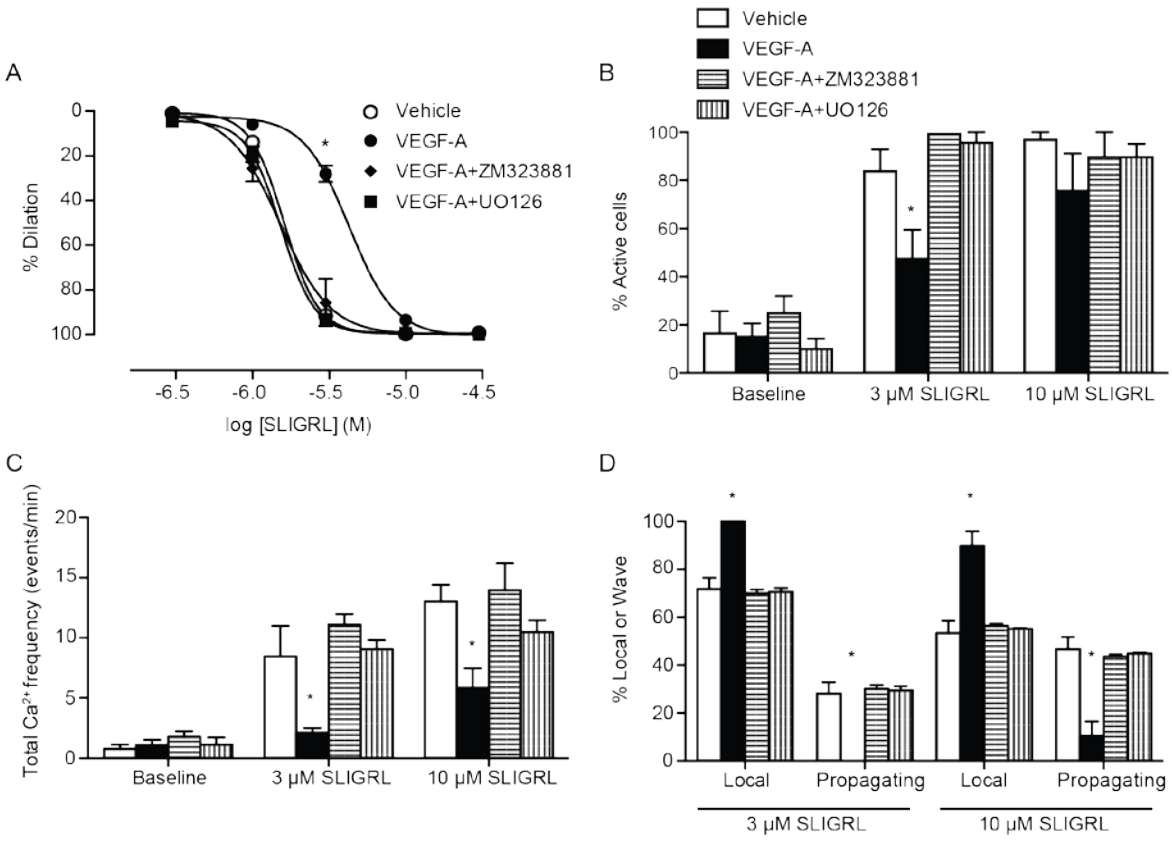

Fig 6. VEGF-A inhibits SLIGRL-mediated EC Ca^{2+} events and vasodilation via ERK1/2 signalling. Vehicle and VEGF-A are from Fig 5. Arteries were perfused with either vehicle or 1 nM VEGF-A with and without inhibitors for 60 min. *A.* ZM323881 and UO126 prevented VEGF-A induced inhibition of SLIGRL-mediated vasodilation (*n* = 3-12). *B-D*, quantification of EC Ca^{2+} activities in arteries treated with ZM323881 or UO126 (*n* = 3-6). **P*<0.05 compared with vehicle.

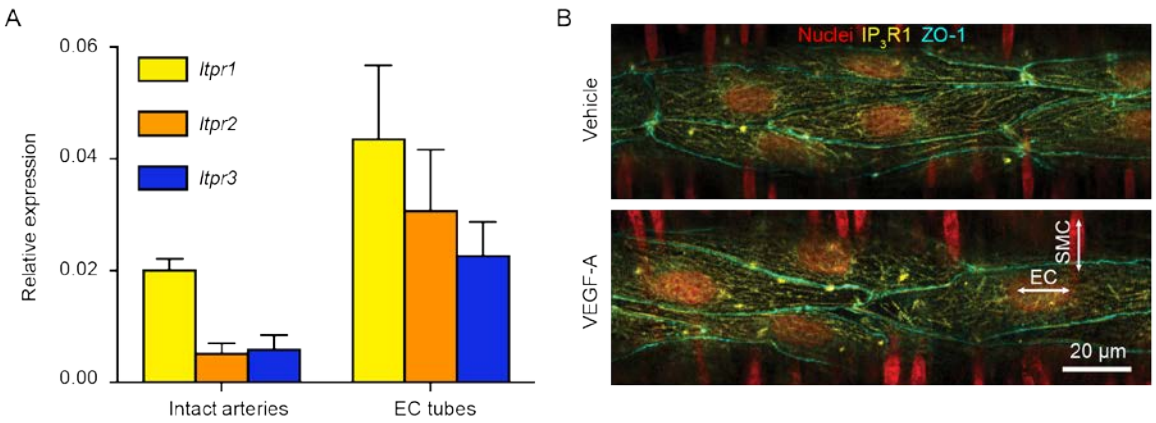

Fig 7. Distribution of IP$_3$R1 in ECs is not modified by VEGF-A. *A.* Itpr1-3 expression in intact arteries and EC tubes (n = 4). *B.* Pressurized arteries were perfused with either vehicle or 1 nM VEGF-A for 60 min. Immuno-labelling showed IP3R1 distribution in ECs (horizontal nuclei). The distribution of ZO-1 appears to be unaltered by VEGF-A in arteries. Representative of 3 arteries per treatment.

References

Bagher, P., Davis, M. and Segal, S. (2011). Visualizing calcium responses to acetylcholine convection along endothelium of arterolar networks in $Cx40^{BAC}$-GCaMP2 transgenic mice, *Am J Physiol Heart Circ Physiol*, **301**, H794-802.

Bai, G.-R., Yang, L.-H., Huang, X.-Y. and Sun, F.-Z. (2006). Inositol 1,4,5-trisphosphate receptor type 1 phosphorylation and regulation by extracellular signal-regulated kinase, *Biochem Biophys Res commun*, **348**, 1319–1327.

Baker, P., Krasnow, J., Roberts, J. and Yeo, K. (1995). Elevated serum levels of vascular endothelial growth factor in patients with preeclampsia, *Obstet Gynecol*, 86, 815–21.

Beleznai, T., Takano, H., Hamill, C., Yarova, P., Douglas, G., Channon, K. and Dora, K. (2011). Enhanced K^+-channel-mediated endothelium-dependent local and conducted dilation of small mesenteric arteries from $ApoE^{-/-}$ mice, *Cardiovasc Res*, **92**, 199–208.

Boeldt, D. S., Krupp, J., Yi, F. X., Khurshid, N., Shah, D. M. and Bird, I. M. (2017). Positive versus negative effects of VEGF165 on Ca2+ signaling and NO production in human endothelial cells, *Am J Physiol Heart Circ Physiol*, **312**, H173–H181.

Boscolo, E., Mulliken, J. B. and Bischoff, J. (2011). VEGFR-1 mediates endothelial differentiation and formation of blood vessels in a murine model of infantile hemangioma, *Am J Pathol*, **179**, 2266–77.

Cheng, H., James, A., Foster, R., Hancox, J. and Bates, D. (2006). VEGF Activates Receptor-Operated Cation Channels in human microvascular endothelial cells, *Arterioscler Thromb Vasc Biol*, **26**, 1768–76.

Dora, K. A., Gallagher, N. T., Mcneish, A. and Garland, C. J. (2008). Modulation of endothelial cell KCa3.1 channels during endothelium-derived hyperpolarizing factor signaling in mesenteric resistance arteries, *Circ Res*, **102**, 1247–1255.

Dora, K., Sandow, S., Gallagher, N., Takano, H., Rummery, N., Hill, C. and Garland, C. (2003). Myoendothelial gap junctions may provide the pathway for EDHF in mouse mesenteric artery, *J Vasc Res*, **40**, 480–90.

Edwards, G., Dora, K., Gardener, M., Garland, C. and Weston, A. (1998). K^+ is an endothelium-derived hyperpolarizing factor in rat arteries', *Nature*, **396**, 269–272.

Egholm, C., Khammy, M. M., Dalsgaard, T., Mazur, A., Tritsaris, K., Hansen, A. J., Aalkjaer, C. and Dissing, X. S. (2016). GLP-1 inhibits VEGFA-mediated signaling in isolated human endothelial cells and VEGFA-induced dilation of rat mesenteric arteries, *Am J Physiol Heart Circ Physiol*, **1311**, 1214–1224.

Favia, A., Desideri, M., Gambara, G., D'Alessio, A., Ruas, M., Esposito, B., Del Bufalo,

D., Parrington, J., Ziparo, E., Palombi, F., Galione, A. and Flippini, A. (2014). VEGF-induced neoangiogenesis is mediated by NAADP, *Proac Natl Acad Sci USA*, **111**, E4706-15.

Fong, G., Rossant, J., Gertsenstein, M. and Breitman, M. (1995). Role of the Flt-1 receptor tyrosine kinase in regulating the assembly of vascular endothelium, *Nature*, **376**, 66–70.

Garland, C. J., Bagher, P., Powell, C., Ye, X., Lemmey, H. A. L., Borysova, L. and Dora, K. A. (2017). Voltage-dependent Ca^{2+} entry into smooth muscle during contraction promotes endothelium-mediated feedback vasodilation in arterioles, *Sci Signal*, **10**, eaal3806.

Goel, H. L. and Mercurio, A. M. (2013). VEGF targets the tumour cell, *Nature reviews. Cancer*, **13**, 871–82.

Grundy, D. (2015). Principles and standards for reporting animal experiments in The Journal of Physiology and Experimental Physiology, *J Physiol*, **593**, 2547–2549.

Hamdollah Zadeh, M., Glass, C. A., Magnussen, A., Hancox, J. and Bates, D. O. (2008). VEGF-mediated elevated intracellular calcium and angiogenesis in human microvascular endothelial cells in vitro are inhibited by dominant negative TRPC6, *Microcirculation*, **15**, 605–614.

Itoh, S., Brawley, L., Wheeler, T., Anthony, F. W., Poston, L. and Hanson, M. A. (2002). Vasodilation to vascular endothelial growth factor in the uterine artery of the pregnant rat is blunted by low dietary protein intake, *Pediatr Res*, **51**, 485–491.

Jang, K., Kim, M., Gilbert, C. A., Simpkins, F., Ince, T. A. and Slingerland, J. M. (2017). VEGFA activates an epigenetic pathway upregulating ovarian cancer-initiating cells, *EMBO Mol Med*, **9**, 304–318.

Kaess, B. M., Preis, S. R., Beiser, A., Sawyer, D. B., Chen, T. C., Seshadri, S. and Vasan, R. S. (2016). Circulating vascular endothelial growth factor and the risk of cardiovascular events, *Heart*, **102**, 1898–1901.

Kawamura, H., Li, X., Harper, S. J., Bates, D. O. and Claesson-Welsh, L. (2008). Vascular Endothelial Growth Factor (VEGF)-A_{165}b Is a Weak In vitro Agonist for VEGF Receptor-2 Due to Lack of Coreceptor Binding and Deficient Regulation of Kinase Activity, *Cancer Res*, **68**, 4683–4692.

Ku, D. D., Zaleski, J. K., Liu, S. and Brock, T. A. (1993). Vascular endothelial growth factor induces EDRF-dependent relaxation in coronary arteries, *Am J Physiol*, **265**, H586-92.

Larsson, A., Sköldenberg, E. and Eericson, H. (2002). Serum and plasma levels of FGF-2 and VEGF in healthy blood donors, *Angiogenesis*, **5**, 107–110.

Lim, H., Blann, A., Chong, A., Freestone, B. and Lip, G. (2004). Plasma vascular

endothelial growth factor, angiopoietin-1, and angiopoietin-2 in diabetes: implications for cardiovascular risk and effects of multifactorial intervention, *Diabetes Care*, **27**, 2918–24.

Losordo, D. W., Vale, P. R., Hendel, R. C., Milliken, C. E., Fortuin, F. D., Cummings, N., Schatz, R. A., Asahara, T., Isner, J. M. and Kuntz, R. E. (2002). Clinical Investigation and Reports Trial of Myocardial Vascular Endothelial Growth Factor 2 Gene Transfer by Catheter Delivery in Patients With Chronic Myocardial Ischemia, *Circulation*, **105**, 2012–2018.

McGuire, J. J., Hollenberg, M. D., Andrade-Gordon, P. and Triggle, C. R. (2002). Multiple mechanisms of vascular smooth muscle relaxation by the activation of proteinase-activated receptor 2 in mouse mesenteric arterioles, *Br J Pharmacol*, **135**, 155–69.

Simons, M., Gordon, E. and Claesson-welsh, L. (2016). Mechanisms and regulation of endothelial VEGF receptor signalling, *Nat Rev Mol Cell Biol*, **17**, 611–625.

Socha, M., Hakim, C., Jackson, W. and Segal, S. (2011). Temperature effects on morphological integrity and Ca^{2+} signaling in freshly isolated murine feed artery endothelial cell tubes, *Am J Physiol Heart Circ Physiol*, **301**, H773-83.

Socha, M. J. and Segal, S. S. (2013). Isolation of Microvascular Endothelial Tubes from Mouse Resistance Arteries, *J Vis Exp*, **25**, e50759.

Soker, S., Takashima, S., Miao, H. Q., Neufeld, G. and Klagsbrun, M. (1998). Neuropilin-1 Is Expressed by Endothelial and Tumor Cells as an Isoform-Specific Receptor for Vascular Endothelial Growth Factor, *Cell*, **92**, 735–745.

Stehr, A., Töpel, I., Müller, S., Unverdorben, K., Geissler, E. K., Kasprzak, P. M., Schlitt, H. J. and Steinbauer, M. (2010). VEGF: A Surrogate Marker for Peripheral Vascular Disease, *Eur J Endovasc Surg*, **39**, 330–332.

Stewart, D. J., Kutryk, M. J. B., Fitchett, D., Freeman, M., Camack, N., Su, Y., Siega, A. Della, Bilodeau, L., Burton, J. R. and Proulx, G. (2009). VEGF Gene Therapy Fails to Improve Perfusion of Ischemic Myocardium in Patients With Advanced Coronary Disease : Results of the NORTHERN Trial, *Mol Ther*, **17**, 1109–1115.

Svedas, E., Islam, K. B., Nisell, H. and Kublickiene, K. R. (2003). Vascular endothelial growth factor induced functional and morphologic signs of endothelial dysfunction in isolated arteries from normal pregnant women, *Am J Obstet Gynecol*, **188**,168–176.

Takahashi, Y., Kitadai, Y., Bucana, C. D., Cleary, K. R. and Ellis, L. M. (1995). Expression of Vascular Endothelial Growth Factor and Its Receptor, KDR, Correlates with Vascularity, Metastasis, and Proliferation of Human Colon Cancer, *Cancer Res*, **55**, 3964–3968.

Tran, M. D. and Neary, J. T. (2006). Purinergic signaling induces thrombospondin-1

expression in astrocytes, *Proc Natl Acad Sci USA*, **103**, 9321–9326.

Whittles, C. E., Pocock, T. M., Wedge, S. R., Kendrew, J., Hennequin, L. F., Harper, S. J. and Bates, D. O. (2002). ZM323881, a Novel Inhibitor of Vascular Endothelial Growth Factor-Receptor-2 Tyrosine Kinase Activity, *Microcirculation*, **9**, 513–522.

Yang, L., Bai, G., Huang, X. and Sun, F. (2006). ERK binds, phosphorylates InsP3 type 1 receptor and regulates intracellular calcium dynamics in DT40 cells, *Biochem Biophys Res Commun*, **349**, 1339–1344.

Yang, R., Bunting, S., Ko, A., Leyt, B., Modi, N., Zioncheck, T., Ferrara, N. and Jin, H. (1998). Substantially attenuated hemodynamic responses to Escherichia coli- derived vascular endothelial growth factor given by intravenous infusion compared with bolus injection, *J Pharmacol Exp Ther*, **284**, 103–110.